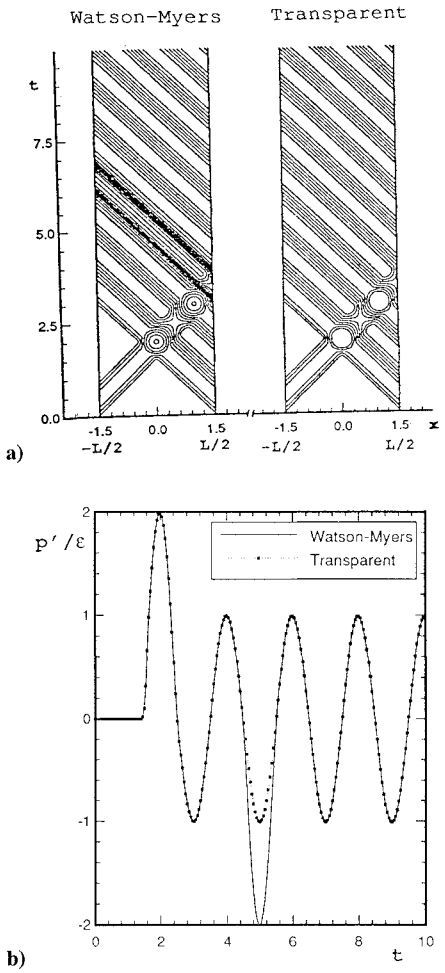

Fig. 2 Tests of nonreflecting property for sound source side at outlet by a wavelet generated at inlet, $M_\infty = 0$: a) x–t diagrams of $p'/\varepsilon, y = H/2$ and b) time histories, $x = 0, y = H/2$.

the computational domain when the actual source is located far downstream.

IV. Conclusion

It can be concluded from the present calculations that the transparent source model proposed here is useful to numerically simulate an acoustic source in the computational domain that is located far downstream. Thus, it is possible to simulate a complex acoustic problem, such as the reflection and transmission of an incident wave. On the other hand, the Watson–Myers' source is a physically existing source, such as a speaker at the boundary. Therefore, care should be taken when choosing acoustic source conditions as well as nonreflecting boundary conditions.

References

[1]Watson, W. R., and Myers, M. K., "Inflow-Outflow Boundary Conditions for Two-Dimensional Acoustic Waves in Channels with Flow," *AIAA Journal*, Vol. 29, No. 9, 1991, pp. 1383–1389

[2]Lee, D. J., and Koo, S. O., "Numerical Study of Sound Generation Due to a Spinning Vortex Pair," AIAA Paper 93-4370, Oct. 1993.

[3]Meadows, K. R., Caughey, D. A., and Casper, J., "Computing Unsteady Shock Waves for Aeroacoustic Applications," AIAA Paper 93-4329, Oct. 1993.

[4]Lele, S. K., "Compact Finite Difference Schemes with Spectral-like Resolution," *Journal of Computational Physics*, Vol. 103, 1992, pp. 16–42.

[5]Roe, P. L., "Technical Prospects for Computational Aeroacoustics," DGLR/AIAA Paper 92-02-032, May 1992.

[6]Bolcs, A., Frasson, T. H., and Platzer, M. F., "Numerical Simulation of Inviscid Transonic Flow Through Nozzles With Fluctuating Back Pressure," *Journal of Turbomachinery*, Vol. 111, April 1989, pp. 169–180.

[7]Thompson, K. W., "Time Dependent Boundary Conditions for Hyperbolic Systems," *Journal of Computational Physics*, Vol. 68, 1987, pp. 1–24.

[8]Yee, H. C., "A Class of High-Resolution Explicit and Implicit Shock-Capturing Methods," NASA TM 101088, Feb. 1989.

[9]Hirsch, C., *Numerical Computation of Internal and External Flows*, 1st ed., Vol. 2, Wiley, New York, 1990, pp. 183, 408–594.

[10]Dowling, A. P., and Ffowcs Williams, J. E., *Sound and Sources of Sound*, 1st ed., Ellis Horwood, West Sussex, England, UK, 1983, pp. 65–69.

Nonequilibrium Anisotropic Eddy–Viscosity/Diffusivity Turbulence Model for Heated Turbulent Flows

Wenyan Ni,* John G. Kawall,† and James F. Keffer‡
University of Toronto,
Toronto, Ontario M5S 1A4, Canada

Introduction

In general, there are two types of turbulence models in use, viz; 1) the standard eddy–viscosity/diffusivity (SEV) model and 2) the Reynolds stress/flux (RS) model.

The SEV model is relatively simple and effective; in addition, it is easy to incorporate into most turbulence computational fluid dynamics (CFD) computer codes. However, it has three major deficiencies: 1) It is subject to the assumption that all normal Reynolds stresses are essentially equal (the isotropic assumption). 2) It is subject to the assumption of local equilibrium, which implies that the eddy–viscosity coefficient is a constant throughout the whole field. 3) It does not account for the effect of buoyancy explicitly.

In contrast, the RS model can account for buoyancy effects, as well as the anisotropy and nonequilibrium properties of turbulence. But, this model (even in its algebraic form) is computationally less efficient than the SEV model and is often numerically unstable.[1]

Because of the deficiencies of the SEV model just noted, considerable research effort has been directed toward the development of a nonlinear eddy–viscosity model.[2] However, these models do not deal with thermal turbulence quantities and do not account for buoyancy effects.

In the present study, a nonequilibrium anisotropic form of the eddy–viscosity/diffusivity turbulence (NAEV) model has been developed for heated turbulent flows. The NAEV model is designed to deal with both the Reynolds stresses and Reynolds heat fluxes with the advantages of numerical efficiency and stability.

Derivation of the Nonequilibrium Anisotropic Eddy–Viscosity Model

The NAEV model is derived from the algebraic second-moment (ASM) model which has the following complete form for determining the Reynolds stresses ($-\overline{u_i u_j}$) and heat fluxes ($-\overline{u_i\theta}$) (see Refs. 2 and 3):

$$-\overline{u_i u_j} = -\tfrac{2}{3}k\delta_{ij} + 2f_\mu c'_{\mu 0}(k^2/\varepsilon)S_{ij} - (k/\varepsilon)f_\mu\left[\alpha_1\left(P_{ij} - \tfrac{2}{3}P\delta_{ij}\right) + \alpha_2\left(C_{ij} - \tfrac{2}{3}P\delta_{ij}\right) + \alpha_3\left(G_{ij} - \tfrac{2}{3}G\delta_{ij}\right)\right] \quad (1)$$

$$-\overline{u_i\theta} = \frac{k}{\varepsilon}f_t\left[\alpha_{t1}\overline{u_i u_j}\frac{\partial T}{\partial x_j} + \alpha_{t2}\overline{u_j\theta}\frac{\partial U_i}{\partial x_j} + \alpha_{t3}\beta g_i\overline{\theta^2}\right] \quad (2)$$

In these two equations, k and ε are the turbulence kinetic energy

Received Sept. 1, 1994; revision received Nov. 22, 1994; accepted for publication Dec. 3, 1994.

*Research Assistant, Department of Mechanical Engineering. Member AIAA.

†Associate Professor, Department of Mechanical Engineering.

‡Professor, Department of Mechanical Engineering.

and its dissipation rate, $S_{ij} = 0.5(\partial U_i/\partial x_j + \partial U_j/\partial x_i)$ is the mean rate-of-strain tensor,

$$P_{ij} = -\left(\overline{u_i u_l}\frac{\partial U_j}{\partial x_l} + \overline{u_j u_l}\frac{\partial U_i}{\partial x_l}\right) \tag{3}$$

$$C_{ij} = -\left(\overline{u_i u_l}\frac{\partial U_l}{\partial x_j} + \overline{u_j u_l}\frac{\partial U_l}{\partial x_i}\right) \tag{4}$$

$$P = -\overline{u_i u_j}\frac{\partial U_i}{\partial x_j} = 0.5P_{jj} = 0.5C_{jj} \tag{5}$$

are the production terms due to the mean flowfield,

$$G_{ij} = -\beta(g_i\overline{u_j\theta} + g_j\overline{u_i\theta}) \tag{6}$$

$$G = -\beta g_j\overline{u_j\theta} = 0.5G_{jj} \tag{7}$$

are the production terms due to the buoyancy,

$$f_\mu = \frac{a_1}{(P+G)/\varepsilon - 1 + a_1} \tag{8}$$

$$f_t = \frac{a_{t1}}{0.5[(P+G)/\varepsilon - 1] + a_{t1}} \tag{9}$$

are the nonequilibrium eddy–viscosity/conductivity correction coefficients, T is the mean temperature, β is the volumetric expansion coefficient, g_i is the component of the gravitation vector in the x_i direction, $\overline{\theta^2}$ is the mean-square temperature, and $c'_{\mu 0}$ and α are model constants. Summation is implied whenever an index is repeated in the same term. The equation of the ASM model for determining $\overline{\theta^2}$ can be obtained as follows[3]:

$$\overline{\theta^2} = -R_t\frac{k}{\varepsilon}\overline{u_j\theta}\frac{\partial T}{\partial x_j} \tag{10}$$

where R_t is assumed to be constant.

As can be seen, the right-hand sides of Eqs. (1) and (2) involve nonlinear terms which are explicit functions of the Reynolds stresses and heat fluxes; moreover, these two equations are coupled. The strong nonlinearity and interdependence of these equations are the source of the deficiencies of the ASM model with respect to computational time and stability. To overcome these deficiencies, without compromising the integrity of the model, the nonlinear terms in Eqs. (1) and (2) need to be modified.

Since P in the SEV model can be approximated by

$$P = \left[-\tfrac{2}{3}(k + \mu_{t0}S_{kk})\delta_{ij} + 2\mu_{t0}S_{ij}\right]\frac{\partial U_i}{\partial x_j}$$

$$= -\tfrac{2}{3}(k + \mu_{t0}S_{kk})S_{ii} + E \tag{11}$$

and since P is the sum of the diagonal terms of tensor P_{ij} (and C_{ij}), it follows that we can approximate P_{ij} and C_{ij} in Eq. (1) by similar expressions to Eq. (11), viz.,

$$P_{ij} = -4/3(k + \mu_{t0}S_{kk})S_{ij} + E_{ij} \tag{12}$$

$$C_{ij} = -4/3(k + \mu_{t0}S_{kk})S_{ij} + F_{ij} \tag{13}$$

In Eqs. (11–13),

$$E = 2\mu_{t0}S_{ij}\frac{\partial U_i}{\partial x_j} \tag{14}$$

$$E_{ij} = 2\mu_{t0}\left(S_{il}\frac{\partial U_j}{\partial x_l} + S_{jl}\frac{\partial U_i}{\partial x_l}\right) \tag{15}$$

$$F_{ij} = 2\mu_{t0}\left(S_{il}\frac{\partial U_l}{\partial x_j} + S_{jl}\frac{\partial U_l}{\partial x_i}\right) \tag{16}$$

serve to describe the anisotropy of turbulence. Based on the preceding idea, the following nonequilibrium anisotropic eddy–viscosity/diffusivity turbulence model for determining the Reynolds stresses is derived from Eq. (1):

$$-\overline{u_i u_j} = -\tfrac{2}{3}(k + \mu_t S_{kk})\delta_{ij} + 2\mu_t S_{ij} - (k/\varepsilon)f_\mu\left[\alpha_1\left(E_{ij} - \tfrac{2}{3}E\delta_{ij}\right) + \alpha_2\left(F_{ij} - \tfrac{2}{3}E\delta_{ij}\right) + \alpha_3\left(G_{ij} - \tfrac{2}{3}G\delta_{ij}\right)\right] \tag{17}$$

In this model, Eq. (17), the buoyancy production term is kept unchanged; also, μ_t is the nonequilibrium Eddy–Viscosity given by

$$\mu_t = c_\mu(k^2/\varepsilon)(1 + c_{\mu 0}(k/\varepsilon)S_{kk}) \tag{18}$$

where $c_\mu = f_\mu c_{\mu 0}$. In a similar manner to that used for deriving Eq. (17), i.e., by substitution of $[\frac{2}{3}(k + \mu_{t0}S_{kk})\delta_{ij} - 2\mu_{t0}S_{ij}]$ and $[(-\mu_{t0}/\sigma_{t0})(\partial T/\partial x_j)]$ for the terms $\overline{u_i u_j}$ and $\overline{u_i\theta}$ on the right-hand side of Eq. (2), respectively, the following equation for determining the Reynolds heat fluxes for a heated turbulent flow is obtained:

$$-\overline{u_i\theta} = \frac{\mu_t}{\sigma_t}\frac{\partial T}{\partial x_i} - \frac{k}{\varepsilon}\left(\frac{\mu_t}{\sigma_t}Q_{ij}\frac{\partial T}{\partial x_j} - \alpha_{t3}f_t\beta g_i\overline{\theta^2}\right) \tag{19}$$

where

$$Q_{ij} = (\alpha_{t1}\sigma_{t0} + \alpha_{t2})\frac{\partial U_i}{\partial x_j} + \alpha_{t1}\sigma_{t0}\frac{\partial U_j}{\partial x_i} \tag{20}$$

is a resultant mean rate of strain and $\sigma_t = f_\mu\sigma_{t0}/f_t$ is the nonequilibrium turbulent Prandtl number. To complete the NAEV model, Eq. (10) for determining $\overline{\theta^2}$ is directly adopted without any change.

Numerical Tests on the Nonequilibrium Anisotropic Eddy–Viscosity Model

To check the efficacy of the NAEV model, two typical turbulent flow cases have been examined[2]: 1) a heated plane air jet issuing into ambient air flow and 2) flow past a backward-facing step.

The Reynolds-averaged Navier–Stokes equations in divergence form are used as the governing equations. These equations are discretized by the finite volume technique and the resulting nonlinear algebraic equations are solved iteratively by a line relaxation method. The computational procedure is based on a modified version of Patankar's SIMPLER method.[2]

A Cartesian x–y coordinate system is used, with flow in the x direction. A grid of 101×51 in the x and y directions, respectively, is used in all cases. The accuracy of the results obtained with this grid was tested by comparing them with the results obtained with a coarser grid of 61×31. The maximum differences between the results based on the two grids are within about 10%, whereas the grid sizes are about 40% different in each direction.[2] Accordingly, the grid of 101×51 is fine enough to provide essentially grid-independent results for both flows.

With the grid of 101×51, for each iteration, the SEV model takes 3.64 s and the NAEV model takes 4.89 s of CPU time on a SUN Sparc II workstation. Thus, the NAEV model requires one-third more CPU time than does the SEV model. About 1600 iterations are needed to achieve convergence. Additional computational details and boundary conditions are reported in Ref. 2.

A. Heated Plane Turbulent Air Jet Flow

The similarity profiles of the Reynolds stresses, heat fluxes, and temperature fluctuations are shown in Fig. 1. It can be seen that for all of the Reynolds stress components the results predicted by the NAEV model are in good agreement with the experimental data of Ramaprian and Chandrasekhara.[4] The RS model used by Malin and Younis[5] predicts values for the axial normal stress $\overline{u^2}$ that are higher than the experimental data, and it predicts the same values for the cross stream and spanwise normal stresses $\overline{v^2}$ and $\overline{w^2}$. The SEV model predicts essentially the same values for the Reynolds normal stresses since it is subject to the isotropic assumption and does not account for buoyancy effects. In the case of the axial turbulent heat flux ($\overline{u\theta}$), the results obtained by the NAEV model

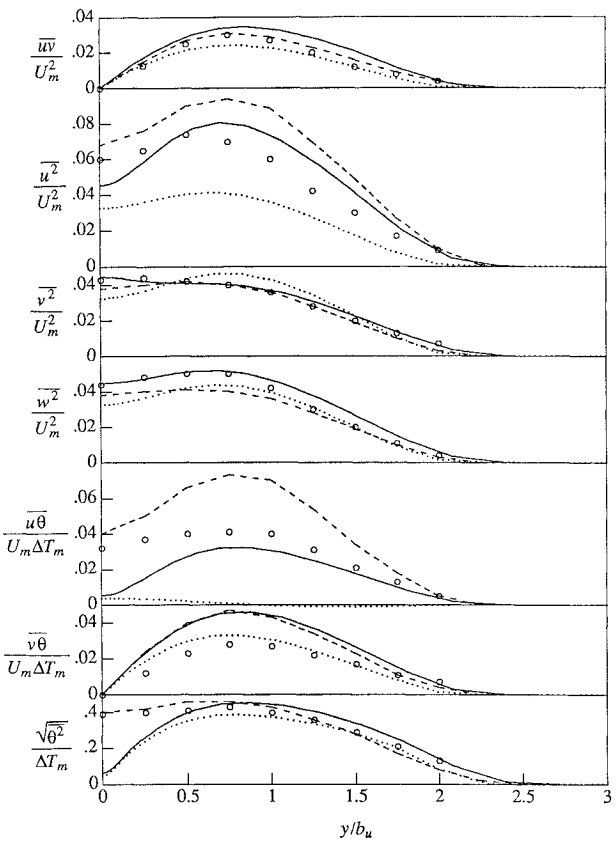

Fig. 1 Similarity profiles of Reynolds stresses, heat fluxes, and temperature fluctuations for a heated jet: — NAEV model, · · · SEV model, - - RS model,[5] o experiment.[4]

show a significant improvement over those obtained by the SEV model but are lower than the experimental data of Ramaprian and Chandrasekhara,[4] whereas the RS model[5] yields much higher results than the experimental data. In the case of the cross stream turbulent heat flux $\overline{v\theta}$ and temperature fluctuations $\overline{\theta^2}$, the three models predict different results, but the results predicted by the NAEV model are closer to those predicted by the RS model,[5] whereas the results of $\overline{v\theta}$ predicted by the SEV model display the closest agreement with the experimental data of Ramaprian and Chandrasekhara.[4]

B. Flow Past a Backward-Facing Step

This flow has served as a primary benchmark for the performance of turbulence models in the prediction of separated flows (e.g., Ref. 6). It is well known that the SEV model substantially underpredicts the reattachment point for this flow. The separation length (L/H, where H is the step height) is predicted by means of the SEV model as 5.7, whereas experiments indicate that it should be about 7.0.

The NAEV model predicts $L/H = 7.0$, which is a significant improvement over the result predicted by means of the SEV model. In comparison, the local equilibrium anisotropic model (i.e., in the NAEV model obtained with $f_\mu = 1$) predicts $L/H = 6.0$, whereas the nonequilibrium isotropic model (i.e., in the NAEV model obtained with $\alpha_1 = \alpha_2 = 0$) predicts $L/H = 7.0$. Thus, we can conclude that, for this flow, the improvement in the predictions of the separation length is essentially due to the fact that the NAEV model accounts for the nonequilibrium effects; the anisotropy of the flow has only a second-order effect.

Concluding Remarks

The NAEV model can effectively account for the nonequilibrium and anisotropic properties of a turbulent shear flow. This model is as equally capable as the RS model of accounting for buoyancy forces when the flow is heated, and it has the same advantages of numerical efficiency and stability as does the SEV model.

Acknowledgment

This research was sponsored by the National Research Council of Canada under Grant A-2746.

References

[1]Huang, P. G., and Leschziner, M. A., "Stabilization of Recirculating-Flow Computations Performed with Second-Moment Closures and Third-Order Discretization," *Proceedings of the Fifth Symposium on Turbulent Shear Flows* (Cornell, NY), 1985, pp. 20.7–20.12.

[2]Ni, W., "Numerical Prediction of the Statistical Properties of Heated Turbulent Air Jets in a Cross-Flow," Ph.D. Thesis, Univ. of Toronto, Canada, 1994.

[3]Rodi, W., *Turbulence Models and Their Application in Hydraulics*, International Association for Hydraulic Research, Delft, The Netherlands, 1980.

[4]Ramaprian, B. R., and Chandrasekhara, M. S., "Study of Vertical Plane Turbulent Jets and Plumes," IIHR 257, Univ. of Iowa, 1983.

[5]Malin, M. R., and Younis, B. A., "Calculation of Turbulent Buoyant Plumes with a Reynolds Stress and Heat Flux Transport Closure," *Journal of Heat and Mass Transfer*, Vol. 33, No. 10, 1990, pp. 2247–2264.

[6]Kim, J., Kline, S. J., and Johnston, J. P., "Investigation of a Reattaching Turbulent Shear Layer: Flow Over a Backward-Facing Step," *Journal of Fluids Engineering*, Vol. 102, Sept. 1980, pp. 302–308.

Shock Wave/Vortex Interaction in a Flow over 90-deg Sharp Corner

Naoki Uchiyama* and Osamu Inoue†
Tohoku University, Sendai 980-77, Japan

Introduction

A SHOCK wave diffraction over a 90-deg sharp convex corner provides one of the most basic flows in the field of compressible fluid dynamics. A variety of diffraction patterns dependent on incident shock Mach number has been extensively studied theoretically, experimentally, and numerically. However, it seems that the evolution process of a vortical flowfield near the corner has not been fully addressed compared to the shock wave diffraction process itself. For example, it is controversial whether or not secondary shock waves appearing in the vortical flowfield have a branch-like structure. Uchiyama and Inoue[1] suggest by computation that the branch-like structure may appear, although in experiments this structure has not been observed so far. This discrepancy may stem from some practical limitations in both experimental and computational studies. In the case of experiment, the characteristic time scale required for detectable growth of shear layer instability is relatively much larger than that for shock wave propagation and, hence, in order to capture distinct phenomena caused by shear layer instability, a pretty wide area of a test section is necessary. In the case of computation, capturing details of the flowfield such as rollup of the shear layer is not an easy task even with recent high-resolution schemes with large numbers of computational cells, since a numerical diffusion mechanism is inherent in any shock capturing scheme. To minimize the effect of numerical diffusion and to capture the vortex motion as accurately as possible under limited computer power, the use of adaptive mesh methods is desirable. In the present study, two-dimensional unsteady Euler computation with adaptive mesh refinement (AMR) algorithm[2] was performed to study the evolution process of a vortical flowfield generated near the corner. The results show that due to the growth of the Kelvin–Helmholtz instability, a

Received Sept. 6, 1994; revision received Feb. 17, 1995; accepted for publication Feb. 26, 1995.

*Graduate Student, Department of Mechanical Engineering, Institute of Fluid Science.

†Professor, Institute of Fluid Science. Member AIAA.